Supporting Information

Development of xanthan gum-based solid desiccants for the extraction of water vapors from humid air

Hemant Mittal[1*], Ali Al Alili[1], Saeed M Alhassan[2], Naved I Malek[3], Md. Didarul Islam[4]

[1]DEWA R&D Center, Dubai Electricity & Water Authority (DEWA), P.O. Box 564, Dubai, United Arab Emirates

[2]Department of Chemical Engineering, Khalifa University of Science and Technology, PO Box 127788, Abu Dhabi, United Arab Emirates

[3]Ionic Liquids Research laboratory, Department of Chemistry, Sardar Vallabhbhai National Institute of Technology, Surat- 07, India

[4]Department of Mechanical Engineering, Khalifa University of Science and Technology, PO Box 127788, Abu Dhabi, United Arab Emirates

*Corresponding authors E-mail: mittal.hemant5@gmail.com (Hemant Mittal)

Chemical structure of Xanthan gum

Xanthan gum is a gram negative yellow pigmented bacterium anionic polysaccharide obtained from the bacterial coat of *Xanthomonas campestris* and is generally produced by fermentation of glucose, sucrose, or lactose by the *Xanthomonas campestris* bacterium. The fermented part is precipitated using isopropyl alcohol, dried, converted into fine powder and added to a liquid medium to form the gum. Xanthan gum has high viscosity even at very low concentrations and is completely soluble in cold as well as hot water.

In the main chain of xanthan gum, pentasaccharide repeating units of D-glucose are joined through the β-1 position of one unit with 4th position of the next unit similar in the chemical structure of cellulose. In the primary structure of *xanthan* gum main chain of (1→4)- linked β -D-glucopyranose units is attached with the trisaccharide side-chains of alternate sugar residues at the C-3 position and the side chain is made up of two mannose residues and a glucuronic acid residue. In the terminal portion β -D-mannopyranose residue is (1→4)- linked β -D-glucuronic acid residue and that in turn is (1→2)- linked to non-terminal α-D-mannopyranose residue (Figure S1) (Li & Feke, 2015). The 6-OH group of the non-terminal D-mannopyranose residue is present as acetic acid ester and the pyruvate acetal groups are located on the D-mannopyranosyl end groups of the side-chains. Modification of polysaccharide chains confirmations and its characteristics depends upon the different glycosidic linkages in the main chain. Pyruvic acid attached to the terminal carbohydrate of the side chains adds another carboxylate group and the different pyruvate levels of xanthan gum have different rheological properties. The main constitutes of xanthan gum are glucose, mannose, glucuronic acid, acetate and pyruvate and they are present in the ratio 37:43.4:19.5:4.5:4.4, respectively (Mittal et al., 2013).
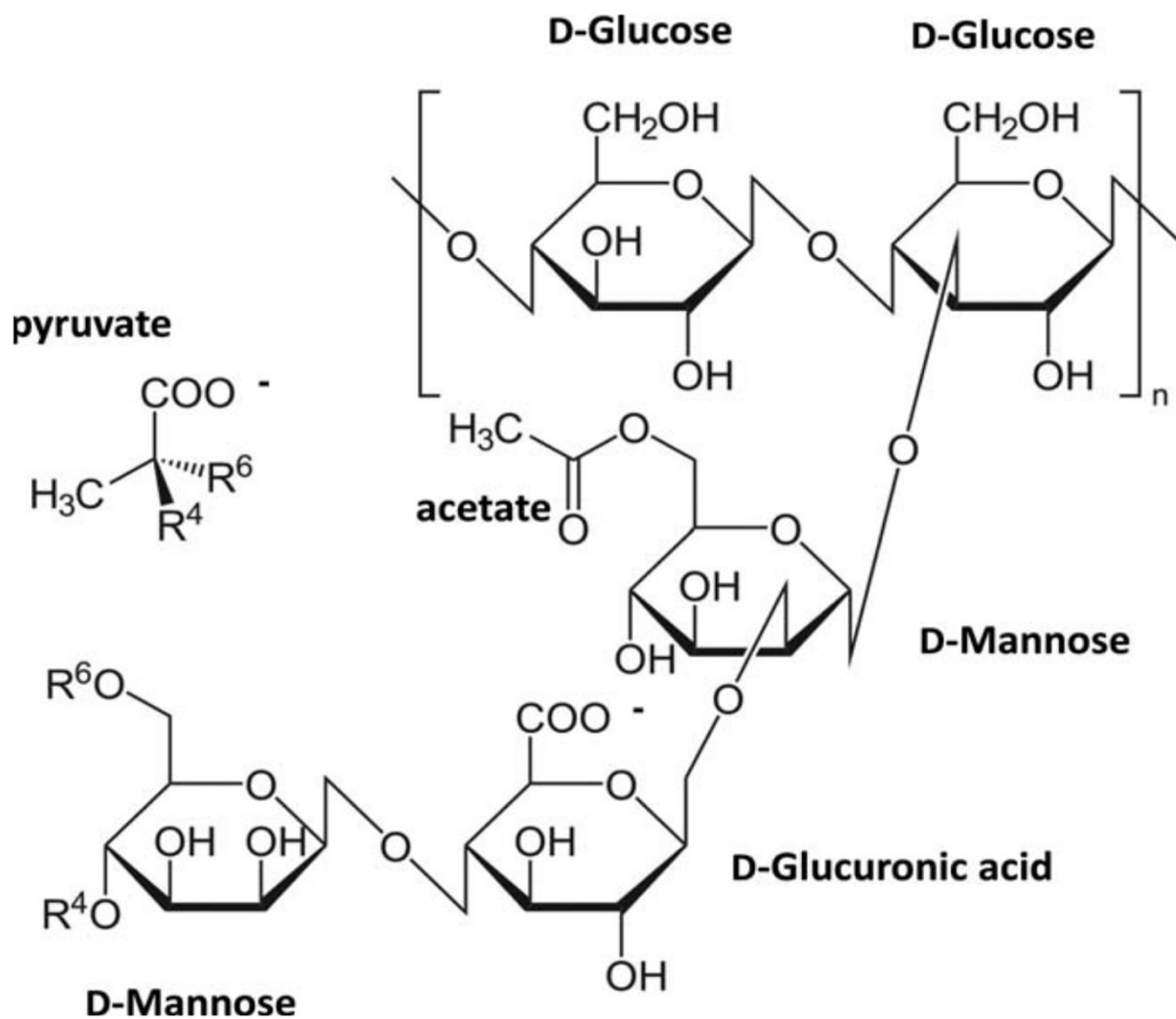
Figure S1: Chemical structure of Xanthan gum (Mittal et al., 2013).

Characterization

Different samples were characterized using different techniques such as scanning electron microscope (SEM) (Quanta FEG 250 SEM, FEI, USA) coupled with energy dispersive X-ray spectroscopy (EDS) and elemental mapping. Before analysis, the samples were coated with gold to induce the conducting effect. The attenuated total reflectance-Fourier transform infrared spectroscopy (ATR-FTIR) spectrum was recorded using Bruker Vertex 70 FTIR spectrophotometer, Germany, in the 4000-400 cm^{-1} spectral range. Thermal analysis of the samples was performed in the temperature range of 50-800ºC with a 10ºC/min rise in temperature using a thermal analyzer (Discovery TGA). XRD of the samples were recorded on X'PERT Powder, PANalytical powder diffractometer (Netherlands) in the Bragg's angle (2θ) ranging from 5-70° and having Cu-Kα radiation source (λ = 1.5406 Å, 45 kV, 40 mA).

Water vapor adsorption isotherm models

Freundlich isotherm

Freundlich adsorption isotherm generally represents a multilayer reversible adsorption. The mathematical expression of Freundlich isotherm is an exponential equation which can be represented as (Moon & Kook Lee, 1983):

$$q = k_F \left(p / p_O \right)^{\frac{1}{n}} \qquad (1)$$

where, q is the water adsorbed, k_F represents Freundlich isotherm constant, p/p_o is relative humidity or pressure and n is adsorption intensity refers to the heterogeneous adsorbent (Moon & Kook Lee, 1983).

BET (Brunauer, Emmett and Teller) isotherm

The BET adsorption isotherm is the most widely studied and applied theoretical adsorption isotherm model, but it is only applicable when the value of p/p_o lies between 0.1 and 0.3. The mathematical equation of BET model is represented as (Foo & Hameed, 2010):

$$q = \frac{q_m c a_w}{(1 - a_w)(1 + (c - 1)a_w)} \qquad (2)$$

where, $a_w = p/p_o$ and represents water activity; q_m represents maximum monolayer adsorption capacity and c represents BET constant related to the heat of adsorption.

GAB (Guggenheim, Anderson and Boer) isotherm

The GAB model developed by Guggenheim, Anderson and De-Boer (Anderson, 1946) is based on the theory of multilayer gas adsorption and it is basically an extension of BET model which can be applied over a much wider range of pressure, i.e. $0.1 \leq p/p_o \leq 0.9$ (Anderson, 1946). The mathematical equation of GAB model can be written as:

$$q = \frac{q_m c_G k_G a_w}{(1 - k_G a_w)(1 - k_G a_w + c_G k_G a_w)} \qquad (3)$$

where, c_G and k_G represents GAB constants related to multilayer and monolayer adsorption. BET and GAB isotherms become identical when the value of GAB constant k_G becomes unity.

FHH (Frenkel-Halsey-Hill) isotherm

FHH model developed by Frenkel, Halsey and Hill (Halsey, 1948) generally represents multilayer adsorption on the flat solid surface and capillary condensation. The mathematical equation of FHH model can be represented as:

$$q = q_m \left[-ln\left(p/p_o\right) \right]^{\frac{-1}{r}} \qquad (4)$$

where, r is FHH constant and $1/r$ represents the nature of interactions between the solid surface i.e. adsorbent, and the vapor or gas. Normally, the value of r for water vapor adsorption on graphite is almost unity. If the value of r is very large, then the interactions between the solid surface and vapor are very specific and limited to the neighborhood of solid surface only. However, if r has a small value, then the interactive forces between solid surface and water

vapor are mainly van der Waals forces which can extend up to a comparatively larger distance (Halsey, 1948).

Water vapor adsorption kinetics

To determine the rate of adsorption, experimental kinetics data was correlated with linear driving force (LDF) model which can be mathematically presented as:

$$q_t = q_\infty \left(1 - e^{-k_{eff}t}\right) \tag{5}$$

Taking natural log and rearranging:

$$-\ln\left(1 - q_t/q_\infty\right) = k_{eff}t \tag{6}$$

The value of mass transfer coefficient (k_{eff} in 1/min) was obtained from the slope of a plot between $-ln(1 - q_t/q_\infty)$ vs t,.

To study the diffusion mechanism of water molecules, the initial 60% experimental data was further fitted to the below given equations:

$$\frac{q_t}{q_\infty} = k_1 t^n \tag{7}$$

Taking natural log of both sides,

$$ln\left(\frac{q_t}{q_\infty}\right) = k + n\, ln(t) \tag{8}$$

The values of n and k (proportionality constant) can be calculated as the slope and intercept of the graph between $ln(q_t/q_\infty)$ and $ln(t)$

Short time fractional uptake method was utilized to calculate the inter-crystalline diffusion coefficient (D) by using the following equation:

$$\frac{q_t}{q_\infty} = 4\left(Dt/\pi r^2\right)^{1/2} - \pi\left(Dt/\pi r^2\right) - \pi/3\left(Dt/\pi r^2\right)^{3/2} \tag{9}$$

By comparing equations (8) and (9) and assuming $n=0.5$:

$$k = 4 \left(\frac{D}{\pi r^2} \right)^{1/2} \tag{10}$$

$$\frac{q_t}{q_\infty} = 4 \left(\frac{Dt}{\pi r^2} \right)^{1/2} \tag{11}$$

The slope of the plot between q_t/q_∞ vs $t^{1/2}$, gives the value of D.

Table S1: Comparison of the water vapors adsorption capacity of XG-SPH with other adsorbents

Adsorbent	Relative humidity (%)	Temperature (°C)	Adsorption capacity (g_w/g_{ads})	Reference
MCM-41	60	24	0.36	(Llewellyn et al., 1995)
Type-A silica gel	100	25	0.40	(Chua et al., 2002)
Type-RD silica gel	93	25	0.45	(Chua et al., 2002)
MCM-48	59	25	0.08	(Oh et al., 2003)
SBA-1	79	25	0.42	(Oh et al., 2003)
SBA-15	67	25	0.14	(Oh et al., 2003)
Zeolite-Y	63	25	0.36	(Wisniewski & Wojsz, 1992)
Zeolite-X	60	23	0.29	(Dzhigit et al., 1971)
Zeolite-4A	63	25	0.20	(Gorbach et al., 2004)
Alumina	67	20	0.14	(Kim et al., 2002)
AA-300 activated alumina	60	26	0.18	(Desai et al., 1992)
PAM hydrogels	80	25	0.32	(Li et al., 2018)
PAM-CNT	80	25	0.38	(Li et al., 2018)
PAA-SPHs	90	25	0.82	(Mittal et al., 2024)
XG-SPH	90	25	1.38	This study

References

Anderson, R. B. (1946). Modifications of the Brunauer, Emmett and Teller Equation. *Journal of the American Chemical Society*, *68*(4), 686–691. https://doi.org/10.1021/JA01208A049/ASSET/JA01208A049.FP.PNG_V03

Chua, H. T., Ng, K. C., Chakraborty, A., Oo, N. M., & Othman, M. A. (2002). Adsorption Characteristics of Silica Gel + Water Systems. *Journal of Chemical and Engineering Data*, *47*(5), 1177–1181. https://doi.org/10.1021/JE0255067

Desai, R., Hussain, M., & Ruthven, D. M. (1992). Adsorption of water vapour on activated alumina. I —- equilibrium behaviour. *The Canadian Journal of Chemical Engineering*, *70*(4), 699–706. https://doi.org/10.1002/CJCE.5450700412

Dzhigit, O. M., Kiselev, A. V., Mikos, K. N., Muttik, G. G., & Rahmanova, T. A. (1971). Heats of adsorption of water vapour on X-zeolites containing Li+, Na+, K+, Rb+, and Cs+ cations. *Transactions of the Faraday Society*, *67*(0), 458–467. https://doi.org/10.1039/TF9716700458

Foo, K. Y., & Hameed, B. H. (2010). Insights into the modeling of adsorption isotherm systems. *Chemical Engineering Journal*, *156*(1), 2–10. https://doi.org/10.1016/J.CEJ.2009.09.013

Gorbach, A., Stegmaier, M., & Eigenberger, G. (2004). Measurement and Modeling of Water Vapor Adsorption on Zeolite 4A—Equilibria and Kinetics. *Adsorption 2004 10:1*, *10*(1), 29–46. https://doi.org/10.1023/B:ADSO.0000024033.60103.FF

Halsey, G. (1948). Physical Adsorption on Non-Uniform Surfaces. *The Journal of Chemical Physics*, *16*(10), 931–937. https://doi.org/10.1063/1.1746689

Kim, J. H., Lee, C. H., Kim, W. S., Lee, J. S., Kim, J. T., Suh, J. K., & Lee, J. M. (2002). Adsorption Equilibria of Water Vapor on Alumina, Zeolite 13X, and a Zeolite

X/Activated Carbon Composite. *Journal of Chemical and Engineering Data*, *48*(1), 137–141. https://doi.org/10.1021/JE0201267

Li, R., & Feke, D. L. (2015). Rheological and kinetic study of the ultrasonic degradation of xanthan gum in aqueous solution: Effects of pyruvate group. *Carbohydrate Polymers*, *124*, 216–221. https://doi.org/10.1016/J.CARBPOL.2015.02.018

Li, R., Shi, Y., Alsaedi, M., Wu, M., Shi, L., & Wang, P. (2018). Hybrid Hydrogel with High Water Vapor Harvesting Capacity for Deployable Solar-Driven Atmospheric Water Generator. *Environmental Science & Technology*, *52*(19), 11367–11377. https://doi.org/10.1021/acs.est.8b02852

Llewellyn, P. L., Schüth, F., Grillet, Y., Rouquerol, F., Rouquerol, J., & Unger, K. K. (1995). Water Sorption on Mesoporous Aluminosilicate MCM-41. *Langmuir*, *11*(2), 574–577. https://doi.org/10.1021/LA00002A036/ASSET/LA00002A036.FP.PNG_V03

Mittal, H., Al Alili, A., & Alhassan, S. M. (2024). Development of high efficacy super-porous hydrogel composites-based polymer desiccants to capture water vapors from moist air. *Adsorption*, *30*(6), 841–857. https://doi.org/10.1007/S10450-024-00463-W/FIGURES/11

Mittal, H., Jindal, R., Kaith, B. S., & Berry, S. (2013). In Vacuo Synthesis of Xanthan-gum-based Hydrogels with Different Vinyl Monomer Mixtures and their Swelling Behaviour in Response to External Environmental Conditions. *Https://Doi.Org/10.1177/204124791300400102*, *4*(1), 19–34. https://doi.org/10.1177/204124791300400102

Moon, H., & Kook Lee, W. (1983). Intraparticle diffusion in liquid-phase adsorption of phenols with activated carbon in finite batch adsorber. *Journal of Colloid and Interface Science*, *96*(1), 162–171. https://doi.org/10.1016/0021-9797(83)90018-8

Oh, J. S., Shim, W. G., Lee, J. W., Kim, J. H., Moon, H., & Seo, G. (2003). Adsorption Equilibrium of Water Vapor on Mesoporous Materials. *Journal of Chemical and Engineering Data*, *48*(6), 1458–1462. https://doi.org/10.1021/JE0301390

Wisniewski, K. E., & Wojsz, R. (1992). Description of water vapor adsorption on various cationic forms of zeolite Y. *Zeolites*, *12*(1), 37–41. https://doi.org/10.1016/0144-2449(92)90007-C